

NeuroSteiner: A Graph Transformer for Wirelength Estimation

Sahil Manchanda*
Indian Institute of Technology Delhi
sahilm1992@gmail.com

Dana Kianfar
Qualcomm AI Research
dkianfar@qti.qualcomm.com

Markus Peschl
Qualcomm AI Research
mpeschl@qti.qualcomm.com

Romain Lepert
Qualcomm AI Research
romain@qti.qualcomm.com

Michaël Defferrard
Qualcomm AI Research
mdeff@qti.qualcomm.com

ABSTRACT

A core objective of physical design is to minimize wirelength (WL) when placing chip components on a canvas. Computing the minimal WL of a placement requires finding rectilinear Steiner minimum trees (RSMTs), an NP-hard problem. We propose NeuroSteiner, a neural model that distills GeoSteiner, an optimal RSMT solver, to navigate the cost-accuracy frontier of WL estimation. NeuroSteiner is trained on synthesized nets labeled by GeoSteiner, alleviating the need to train on real chip designs. Moreover, NeuroSteiner’s differentiability allows to place by minimizing WL through gradient descent. On ISPD 2005 and 2019, NeuroSteiner can obtain 0.3% WL error while being 60% faster than GeoSteiner, or 0.2% and 30%.

1 INTRODUCTION

Optimizing the placement of circuit elements, e.g., standard cells, in integrated circuits is a critical step in early phases of Electronic Design Automation (EDA) [5, 11, 23]. A placer optimizes the location of circuit elements based on power, performance, and area (PPA) objectives. One crucial objective is *wirelength* (WL), which is a common proxy for power consumption [4, 17, 23]. In principle, a WL function estimates the expected total length of wires needed to connect all nets in a routed netlist. Due to the iterative nature of (gradient-based) placement optimization, any desirable WL function needs to be fast to evaluate, accurate, and differentiable.

Among popular WL estimation methods [11, 23], the Rectilinear Steiner Minimum Tree (RSMT) [11] is known to be an accurate estimator of the true routed WL [22]. Specifically, solving for an RSMT consists of adding nodes—the Steiner points—to a graph such that the length of its spanning tree is minimal with respect to the L1 (Manhattan) metric. While GeoSteiner [10], an algorithm that enumerates Steiner trees, is optimal, its runtime is exponential in the size of the problem (i.e., the net degree) since finding the optimal set of Steiner points for an arbitrary point set in a plane is NP-hard [29].

Several works have used efficient and heuristic approximations to the RSMT with desirable empirical performance. The Minimum Spanning Tree (MST) can be viewed as the simplest approximation because it assumes no Steiner points and incurs a runtime cost of order $O(d \log d)$ for a net of degree d . However, it overestimates WL by 4% on average [25]. Similarly, FLUTE [25] uses a

look-up table to quickly approximate WL without solving for any Steiner points, but is non-differentiable with respect to pin locations. Bi1S [12] proposes a batched-iterative approach to solving the RSMT problem. However, its performance is subpar on low-degree nets which constitute the majority of real-world netlists [5]. Another method SFP [6] leverages CPU/GPU parallelization to accelerate the RSMT construction. Despite its high throughput, its solution quality rapidly degrades with net degree.

While these algorithms were hand-engineered to trade off accuracy for runtime, machine learning (ML) offers an automatic way to navigate this trade-off through the distillation of an optimal algorithm. Moreover, fine-tuning the neural model allows for tailoring it to the real data distribution (not the worst case). Accordingly, there has been a surge in developing ML approximations to combinatorial optimization problems on graphs [3, 7, 13, 15]. Finally, while progress in hardware benefits all workloads, the current emphasis on ML accelerates these workloads faster: GPUs are being optimized for calculations used by neural models.

To our knowledge, REST [16] is the only method that approached the RSMT problem with ML. REST uses a reinforcement learning (RL) approach, proposing an auto-regressive model that sequentially adds edges to a tree to predict an RSMT. However, REST learns multiple models that are specialized for nets of particular degrees (number of pins in a net) instead of a single model for all input sizes. Furthermore, due to its auto-regressive nature, it generates solutions in a step-by-step sequential fashion which can increase runtime. Overall, this can lead to long runtime when predicting the wirelength of a whole netlist, consisting of a large variety of net degrees.

1.1 Contributions

One-shot supervised binary node classification task. We formulate the prediction of Steiner points as a *supervised* binary node-classification task where each intersecting point in the Hanan grid (see Figure 1) is considered as a node in a graph. NeuroSteiner leverages a Graph Transformer [21] through training on labeled data from GeoSteiner [10]. The prediction of Steiner points is done in a *one-shot* fashion, facilitating the utilization of GPU parallelization. In contrast to REST, we only predict Steiner points and not a tree. Thus, we propose a hybrid method, where the neural network focuses on approximating the NP-hard problem of finding Steiner point(s), while the MST calculation can be done in polynomial time.

Training on infinitely available synthetic nets. As obtaining large amounts of industrial chip designs is expensive, we train NeuroSteiner on synthetically-generated labelled data that is cheaper

*Work completed during an internship at Qualcomm AI Research. Qualcomm AI Research is an initiative of Qualcomm Technologies, Inc.



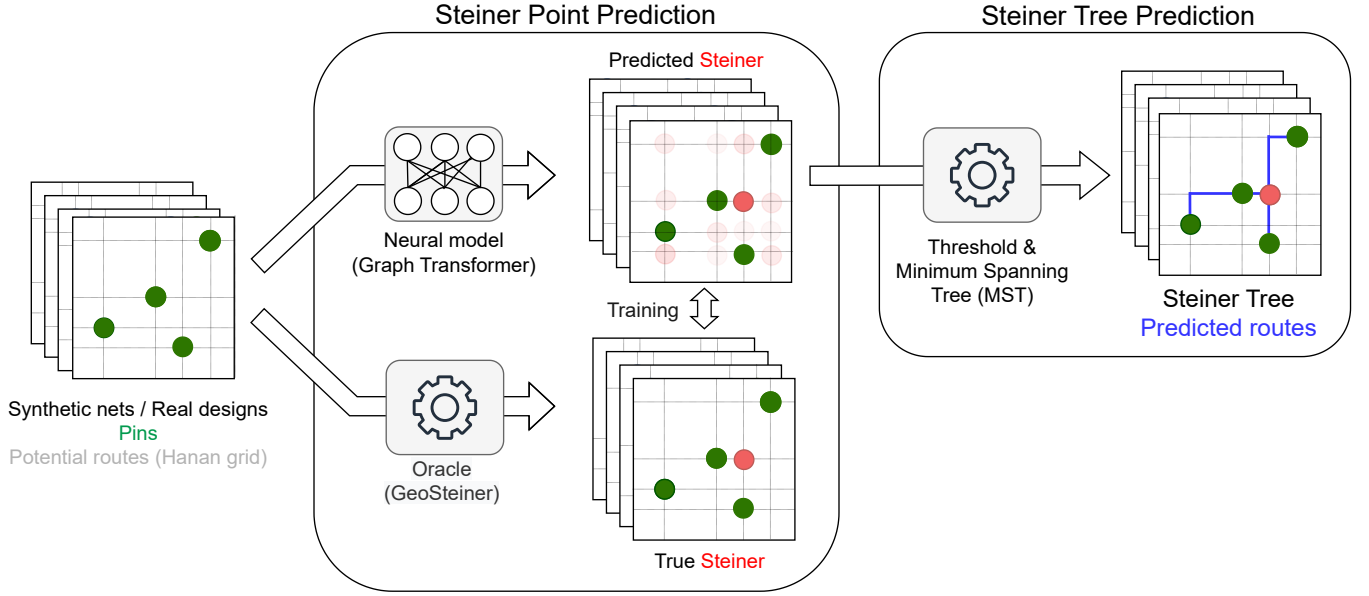


Figure 1: NeuroSteiner. Rectilinear Steiner Minimum Trees (RSMTs), hence wirelength (WL), are predicted in two steps: (1) determine Steiner points, then (2) find its Minimum Spanning Tree (MST). Our neural model predicts the probability that each node on the Hanan grid is a Steiner point. The model is trained by distilling an oracle: synthesized nets (or real designs) are labelled by GeoSteiner, an optimal RSMT solver.

to obtain. We show that the performance of NeuroSteiner can then be improved by fine-tuning on industrial datasets to adapt to the real data distribution.

Evaluation on real-world benchmarks. Through extensive experiments on chip design benchmarks from ISPD2005 and ISPD2019, we establish that NEUROSTEINER (1) constructs an RSMT estimate with an error of about 0.3% when compared to the optimal solution and (2) predicts RSMTs for the benchmarks at 0.3 milliseconds per net on average.

2 METHODOLOGY

Formally, our goal is to solve the following problem:

PROBLEM 1 (RECTILINEAR STEINER MINIMUM TREE). *Given a set of points $\mathcal{V}_P \in \mathbb{R}^2$, construct a rectilinear minimum spanning tree connecting a set of points $\mathcal{V} \in \mathbb{R}^2$, with $\mathcal{V} \supseteq \mathcal{V}_P$.*

In the above definition, the newly introduced points $\mathcal{V} \setminus \mathcal{V}_P$ are called Steiner points. Constructing the Rectilinear Steiner Minimum Tree (RSMT) for a set of points is known to be NP-complete [5, 8]. However, one can show that for any set \mathcal{V}_P , there always exists a set of optimal Steiner points on the Hanan grid [8], which is the union of nodes resulting from intersecting all horizontal and vertical lines passing through each point $v \in \mathcal{V}_P$. For example, Fig. 1 shows green nodes which depict the set of pins on the 2D plane and the lines crossing the green points represent the Hanan grid. Let \mathcal{V}_H denote Hanan points, i.e., the set of intersecting points apart from the pins. We model the RSMT problem as a binary classification problem of the points in \mathcal{V}_H .

PROBLEM 2. *Given a set of pins $\mathcal{V}_P \subseteq \mathbb{R}^2$ and corresponding Hanan points $\mathcal{V}_H \subseteq \mathbb{R}^2$, learn the parameters of a neural model for predicting Steiner points in \mathcal{V}_H .*

Fig. 1 shows the prediction and training flow of NeuroSteiner.

2.1 Hanan grid graph

Given a set of pin points \mathcal{V}_P , we first identify its Hanan points \mathcal{V}_H . To represent relationships among various points in a Hanan grid, we represent the grid using a graph. Let the graph $\mathcal{G} = (\mathcal{V}, \mathcal{E})$ be the graph consisting of the node set $\mathcal{V} = \mathcal{V}_H \cup \mathcal{V}_P$ and the set of edges \mathcal{E} consisting of the Hanan grid. Formally, let $\mathcal{E} = \{e_{uv} = (u, v) \mid v \in \mathcal{N}(u)\}$ be defined as the set of neighboring edges, where neighbors are defined as follows:

DEFINITION 1 (NEIGHBORHOOD OF A NODE). *In a graph \mathcal{G} , a node v is said to be a neighbor of node u , i.e., $v \in \mathcal{N}(u)$, if and only if one of the following conditions hold $\forall w \in \mathcal{V} \setminus \{u, v\}$ and $\forall \alpha, \beta \in [0, 1]$:*

$$v_x = u_x \text{ and } w_x \neq \alpha \cdot v_x + (1 - \alpha) \cdot u_x, \quad (1)$$

$$v_y = u_y \text{ and } w_y \neq \beta \cdot v_y + (1 - \beta) \cdot u_y, \quad (2)$$

where v_x refers to the x coordinate of node v and v_y refers to its y coordinate.

In simple terms, eq. 1 holds if two nodes u and v lie on the same horizontal line and no other node lies horizontally between them. Eq.2 can be viewed analogously for the vertical dimension.

2.2 Node and edge features

Apart from \mathcal{G} , we define a set of node and edge features containing task-relevant information to be used as input to our neural network.

As *node features*, we make use of positional information and a node pin indicator variable. Formally, the input features of a node v are defined as

$$\mathbf{h}_v^0 = [v_x, v_y, I(v)]. \quad (3)$$

In the above equation, v_x and v_y denote the x and y coordinates of a node v , and $I(v)$ is an indicator function that returns 1 if $v \in \mathcal{V}_P$ and 0 otherwise. The coordinates v_x and v_y serve as positional information, which assists our model to recognize spatial dependencies between different nodes [21]. Since our Graph Transformer model employs message-passing between different nodes to construct node embeddings, we employ the pin indicator $I(v)$ as a mechanism for messages to differentiate pin nodes $v \in \mathcal{V}_P$ from candidate Steiner nodes $v \in \mathcal{V}_H$. Let $\mathbf{X}^0 = [\mathbf{h}_v^0]_{v \in \mathcal{V}} \in \mathbb{R}^{|\mathcal{V}| \times 3}$ denote the input feature matrix of nodes belonging to the graph \mathcal{G} .

For the *edge features* of an edge $e_{uv} \in \mathcal{E}$, we define

$$\mathbf{e}_{uv} = [u_x - v_x, u_y - v_y] \quad (4)$$

to capture the displacement between two neighboring nodes on the Hanan grid.

2.3 Message-passing and Graph Transformers

From the input node features, we aim to generate a richer representation that encodes local and global structural information. Since classification of a node as a Steiner point is influenced by nodes beyond its local neighborhood, we need a model that can capture long-range dependencies. While, theoretically, message passing neural networks (MPNNs) [21, 27] are able to learn global interactions, they require several rounds of message-passing at the risk of oversquashing and oversmoothing [18, 20, 27]. Instead, we opt for Graph Transformers, combining MPNNs with a global attention mechanism [24]. This facilitates capturing interactions at both local and global levels [21].

More precisely, we use the GraphGPS [21] Graph Transformer. In GraphGPS, one can use any type of MPNN to aggregate information from the local neighborhood of a target node. Here, we use GINE [26], updating the node embeddings $\mathbf{h}_v^{(l)}$ at layer l by

$$\mathbf{h}_v^{(l+1)} = \text{MLP}^{(l)} \left(\mathbf{h}_v^{(l)} + \sum_{u \in \mathcal{N}(v)} \phi(\mathbf{h}_v^{(l)} + \mathbf{e}_{vu}) \right), \quad (5)$$

where $\phi : \mathbb{R} \rightarrow \mathbb{R}$ is an activation function, in our case chosen to be the ReLU activation $\phi(z) = \max\{0, z\}$. The edge features \mathbf{e}_{uv} are projected to the same dimension as \mathbf{h}_v using an MLP layer. At a given layer l , the above equation aggregates features of neighboring nodes and features of their associated edges. This information is used to generate local embeddings of nodes at layer $l+1$ represented by $\mathbf{X}_{\text{loc}}^{(l+1)} = [\mathbf{h}_v^{(l+1)}]_{v \in \mathcal{V}}$.

For the global attention scheme, we process the node embeddings at layer l as follows

$$\mathbf{Q} = \mathbf{X}^{(l)} \mathbf{W}_Q, \quad \mathbf{K} = \mathbf{X}^{(l)} \mathbf{W}_K, \quad \mathbf{V} = \mathbf{X}^{(l)} \mathbf{W}_V, \quad (6)$$

$$\mathbf{X}_{\text{glob}}^{(l+1)} = \text{softmax}(\mathbf{A}) \mathbf{V} \quad \text{where} \quad \mathbf{A} = \frac{\mathbf{Q} \mathbf{K}^T}{\sqrt{d}}. \quad (7)$$

The input features $\mathbf{X}^{(l)}$ at layer l are projected by three learnable matrices $\mathbf{W}_Q^l \in \mathbb{R}^{d \times d}$, $\mathbf{W}_K^l \in \mathbb{R}^{d \times d}$, and $\mathbf{W}_V^l \in \mathbb{R}^{d \times d}$ to the corresponding representations $\mathbf{Q}, \mathbf{K}, \mathbf{V}$ and the attention matrix

$\mathbf{A} \in \mathbb{R}^{|\mathcal{V}| \times |\mathcal{V}|}$ captures the attention weight between all pairs of nodes.

From the local and global node representations at layer l , their representation at the next layer are given by

$$\mathbf{X}^{(l+1)} = \text{MLP} \left(\mathbf{X}_{\text{loc}}^{(l+1)} + \mathbf{X}_{\text{glob}}^{(l+1)} \right). \quad (8)$$

With GraphGPS, we perform L rounds of local message-passing and global attention to obtain the final representation $\mathbf{X}^{(L)}$ of all nodes in \mathcal{G} . The more the layers, the more complex relationships GraphGPS can capture. Finally, embeddings pass through an MLP to obtain the logits

$$\hat{\mathbf{Y}} = \text{MLP}_{\text{out}} \left(\mathbf{X}^{(L)} \right) \in \mathbb{R}^{|\mathcal{V}|}. \quad (9)$$

These logits represent the probability that a node is a Steiner point.

2.4 Training

The parameters of the model are learned by minimizing an objective that encourages the GraphGPS neural model to predict the true labels \mathbf{Y} . The binary cross-entropy objective is calculated as

$$-\frac{1}{N} \sum_{i=1}^N Y_i \cdot \log \hat{Y}_i + (1 - Y_i) \cdot \log(1 - \hat{Y}_i), \quad (10)$$

$\mathbf{Y} \in \{0, 1\}^N$ are the true labels, $\hat{\mathbf{Y}} \in \mathbb{R}^N$ are the predicted logits, and N is the number of Steiner candidates in the Hanan grid. We note that this loss models each nodes as an independent Bernoulli random variable.

2.5 Inference

After training, for an unseen problem instance we (1) predict the probability of each node in the Hanan grid to be a Steiner point with our Graph Transformer, (2) classify Steiner points by thresholding¹, and (3) obtain the RSMT by finding the Minimum Spanning Tree (MST) from the original pins and predicted Steiner points. Wirelength is computed by the sum length of edges in the RSMT.

3 EXPERIMENTS

In this section, we benchmark the performance of NeuroSteiner against several existing methods on real chip designs. We aim to answer the following questions:

Sec. 3.2 How does NeuroSteiner perform in terms of *wirelength (WL) estimation error* (accuracy) and *runtime* (cost)?

Sec. 3.3 What is the impact of training on synthetic or real nets?

Sec. 3.4 How to explore the cost–accuracy frontier with model capacity?

3.1 Setup

To get a sense of the cost–accuracy frontier, we evaluate NeuroSteiner at two capacities: *small* with $L = 10$ layers and *large* with $L = 20$. At both capacities, our GraphGPS model features hidden representations of size $d = 64$ and one attention head. On our setup, our large model is trained with a batch size of 12 while the small model can afford 16. We train it with the Adam optimizer [14]

¹Nodes whose score \hat{Y}_i are greater than the threshold are classified as Steiner points.

with a learning rate of 10^{-4} and an L2 decay of 10^{-5} . We use a prediction threshold of 0.3 which was decided based upon a held out synthetically generated dataset. All experiments are run on a Linux-based workstation made of an Intel Xeon W-2225 with 32 GB of memory and an NVIDIA GeForce RTX 3080 with 10 GB of memory. We implemented our neural network in PyTorch and used a C++ implementation of MST [1].

Synthetic nets. The synthetic nets used for training are generated by sampling N points (as pins) uniformly at random in the 2D plane, where $N \sim \text{Uniform}(5, 30)$. We trained our model on 50 million such nets. Labels, i.e., the optimal set of Steiner points for these samples, were obtained using GeoSteiner [10].

Real nets. We evaluate performance on real netlists from the ISPD 2005 [19] and 2019 [2] benchmarks. These netlists are made from about 1,000 to 400,000 nets. After filtering for nets with degree larger than 2 and smaller than or equal to 64, the median net degree is 4 and the mean degree is about 7. More statistics about these netlists are shown in Table 5 in Appendix A.

Baselines. We benchmark NeuroSteiner against several methods: GeoSteiner [10] as an optimal solver, a plain Minimum Spanning Tree (MST) as the simplest approximation, BiS [12] as a representative heuristic, and REST [16] as the only neural alternative. GeoSteiner gives a lower-bound on WL estimation—MST an upper-bound. REST is a deep reinforcement learning method that comes in two variants: $T = 1$ and $T = 8$, where T is the number of performed augmentations (i.e., $T = 8$ applies rotations and flips to all nets), a hyper-parameter to be set at inference time. T trades off accuracy with cost: lower values of T result in faster but less accurate predictions. We use the source-code released by the authors of REST in PyTorch (Python), and standard implementations of BiS, GeoSteiner, and MST [1] in C++.

3.2 Results

WL estimation error. Table 1 shows the WL estimation error obtained by different methods against the minimal WL (given by GeoSteiner). While NeuroSteiner doesn’t reach the performance of well-engineered heuristics, it improves on the faster variant of REST ($T = 1$), the only neural alternative. While REST with augmentations ($T = 8$) achieves significantly better performance than our large model, it targets a corner of the cost–accuracy frontier. However, for WL estimation in placement optimization, we expect errors within the 1% range to be sufficiently low. Hence we focused on achieving a fast model below the 1% error mark.

Table 3 breaks down the estimation error per net degree. We observe that the error of all methods grow with net degree. Both NeuroSteiner and REST with $T = 8$ match BiS on nets of small degree, which dominate real netlists (as shown in Table 5).

Runtime. Table 2 shows the time required by different methods to estimate WL. The duration of initial data processing is not included as it is shared amongst all methods. For NeuroSteiner, we report the total runtime: the forward pass of the neural model followed by the MST algorithm. We note that the difference between the runtimes of REST that we report and the ones the authors report [16] is due to potential differences in model loading and batching. Namely,

model→ netlist↓	MST	BiS	REST		NeuroSteiner	
			$T = 1$	$T = 8$	small	large
test1	7.298	0.067	0.423	0.108	0.715	0.503
test2	7.760	0.045	0.224	0.044	0.324	0.237
test3	7.940	0.047	0.298	0.026	0.237	0.132
test4	4.033	0.015	0.073	0.007	0.387	0.289
test5	5.913	0.028	0.247	0.027	0.777	0.557
test6	8.167	0.046	0.218	0.044	0.333	0.243
test7	7.937	0.050	0.224	0.044	0.330	0.239
test8	7.875	0.047	0.216	0.041	0.317	0.229
test9	7.942	0.048	0.223	0.044	0.328	0.237
test10	7.832	0.047	0.220	0.042	0.322	0.230
adaptec1	7.271	0.060	0.330	0.046	0.298	0.206
adaptec2	7.133	0.064	0.385	0.065	0.349	0.250
adaptec3	6.921	0.054	0.412	0.068	0.318	0.252
adaptec4	7.097	0.051	0.396	0.067	0.289	0.238
bigblue1	7.195	0.063	0.443	0.053	0.291	0.190
bigblue2	6.676	0.054	0.261	0.040	0.264	0.176
bigblue3	7.451	0.063	0.440	0.068	0.319	0.247
overall	7.430	0.052	0.294	0.050	0.317	0.232

Table 1: Wirelength (WL) estimation error (%) against the optimal (GST). The reported error is the average across all nets, per netlist and overall. Lower is better.

model→ netlist↓	GST	MST	BiS	REST		NeuroSteiner	
				$T = 1$	$T = 8$	small	large
test1	0.93	0.02	2.05	98.01	111.59	1.00	0.55
test2	15.38	0.41	14.20	112.61	133.72	16.61	9.50
test3	0.37	0.03	1.43	83.71	94.66	0.81	0.47
test4	2.10	0.75	8.14	50.91	60.45	3.84	2.73
test5	0.41	0.05	1.71	81.30	92.09	0.93	0.57
test6	81.30	1.29	72.04	115.22	144.70	38.54	21.45
test7	162.16	3.16	150.72	117.99	158.01	77.18	44.74
test8	115.93	4.43	155.37	117.09	171.28	123.97	69.91
test9	415.69	7.50	324.28	116.06	189.92	207.50	111.91
test10	412.05	6.00	329.49	116.09	190.06	196.39	110.67
adaptec1	54.73	1.80	44.15	109.32	139.14	47.30	25.35
adaptec2	75.10	1.88	97.23	111.92	143.32	72.44	40.13
adaptec3	133.63	2.46	148.02	113.30	154.88	124.73	67.31
adaptec4	133.84	2.36	137.12	114.16	157.15	122.22	67.77
bigblue1	61.60	2.03	47.87	111.55	143.39	51.81	29.07
bigblue2	99.50	3.59	135.59	114.17	155.60	88.56	48.20
bigblue3	196.52	5.42	232.36	115.69	174.56	169.87	91.84
per net	770	17	790	720	970	300	540

Table 2: Total runtime per netlist in seconds, and the mean per net in microseconds. Lower is better.

since REST uses different model checkpoints for different degrees, we evaluate different degree nets on different checkpoints, which have been provided for every 5 degrees by the authors. We then report the inference runtime of REST for sequentially processing

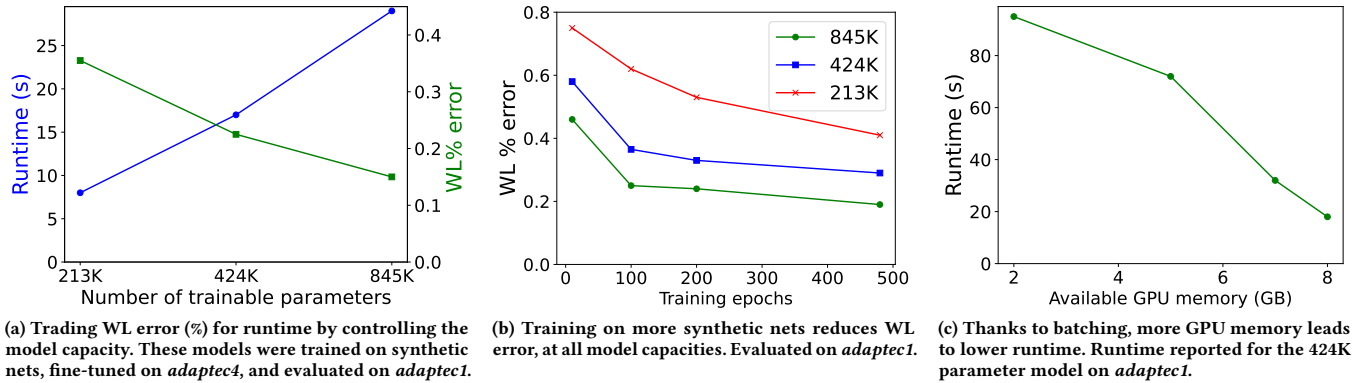


Figure 2: Scaling properties.

model → degree ↓	MST	BI1S	REST		NeuroSteiner	
			T = 1	T = 8	small	large
3–9	6.79	0.03	0.25	0.02	0.07	0.03
10–19	7.38	0.17	0.58	0.07	0.83	0.57
20–29	8.26	0.25	1.22	0.30	1.94	1.59
30–39	8.42	0.26	1.82	0.54	2.79	2.46
40–49	7.32	0.20	3.47	1.11	3.72	4.21
50–59	7.12	0.18	4.74	1.75	4.50	5.14
60–64	7.21	0.19	5.36	2.12	4.40	5.65

 Table 3: Wirelength (WL) estimation error (%), averaged over *adaptec3* nets, grouped by degree.

model	test netlist	training nets		
		adaptec4	synthetic	both
large	adaptec1	0.351	0.194	0.159
small	adaptec3	0.533	0.318	0.290

 Table 4: Wirelength (WL) estimation error (%) for different training strategies: training on *adaptec4* only, training on synthetic nets only, or training on synthetic nets then fine-tuning on *adaptec4*. Lower is better.

batches of same-degree nets on the corresponding checkpoint for the closest multiple of 5. We observe that in most cases NeuroSteiner is faster than REST. We also observe a constant runtime overhead for REST, which we attribute to the sequential nature of degree-based batching and prediction. On the other hand, for NeuroSteiner, we divide nets into 5 groups of similar degrees. For each group, we use an optimized batch size, fitting as many nets as possible into a single forward pass.

3.3 Fine-tuning on real nets

In section 3.2, we showed that training on synthetic nets achieves good results on real-world benchmarks without further fine-tuning,

alleviating the need to train on scarce real designs. If one nonetheless has access to relevant netlists—for example previous versions of the same design—training on them can improve accuracy [28] due to a lower discrepancy between the training and testing nets.

Table 4 shows the WL estimation error for different training strategies.² Training on synthetic nets is better than training on a single real design. With many parameters, our model has the capacity to overfit smaller datasets and to fail generalizing to different test datasets. This emphasizes the importance of training on many synthetic nets (see also Figure 2b).

However, training on synthetic then real nets, i.e., training then fine-tuning, shows a significant improvement (especially with the larger model). This suggests that while synthetic training makes the model learn the fundamentals, fine-tuning enables tailoring to the real data distribution, without overfitting. As a result, we expect training on cheap synthetic nets then fine-tuning on scarce real nets to further improve on the performance reported in Table 1.

3.4 Scaling properties

Cost–accuracy tradeoff. Figure 2a shows the runtime and WL estimation error obtained by NeuroSteiner for different model capacities (number of trainable parameters). As the number of parameters increase, the error decreases and the runtime increases—allowing for an easy control of the cost–accuracy tradeoff.

More data. Figure 2b shows how training on more synthetic nets reduces the WL estimation error till convergence.

Parallelism. As NeuroSteiner, unlike REST, can process nets of different degree simultaneously, increasing GPU memory allows for more nets to be processed simultaneously, irrespective of a netlist’s degree distribution. Figure 2c shows that the runtime of NeuroSteiner indeed decreases linearly as GPU memory increases.

4 CONCLUSION

We introduced NeuroSteiner, a Graph Transformer neural model, to predict the Steiner points on a Hanan grid graph in *one shot*. Wirelength (WL) is then estimated through the construction of Rectilinear Steiner Minimum Trees (RSMTs).

²These are not comparable to the errors reported in Table 1.

Discussion. Although NeuroSteiner achieves high performance at faster runtime when compared to GeoSteiner, we acknowledge that heuristics, such as SFP, for computing the RSMT can achieve competitive performance and prediction speed through efficient implementations. This is common in the ML for combinatorial optimization literature [9]. However, algorithms, such as GeoSteiner, Bi1S, or SFP make discrete choices in order to generate Steiner points, impairing differentiability and often fixing a single tradeoff in terms of speed and accuracy. In this work, we aim to advance the frontier of ML-based methods for approximating the RSMT. We show that, compared to the state-of-the-art neural baseline REST, NeuroSteiner is able to achieve a competitive solution quality while requiring only a single neural model. This has potential advantages in terms of inference speed and memory requirements. Furthermore, we show that NeuroSteiner can be fine-tuned to a task-specific data distribution (Section 3.3), allowing for further performance improvements when iterating through netlist revisions.

Future Work. To simplify modeling, we treated each Steiner point independently during training and inference. Since the Steiner point problem is inherently combinatorial, future work could explore joint or conditional Steiner points models to further enhance the quality of predictions. Furthermore, our proposed method first predicts the Steiner points and then computes MST to obtain wirelength. An alternative to this approach is to use a neural network to directly predict the wirelength of RSMT by treating it as a regression task. This alternative promises faster execution time and an end-to-end differentiable path from wirelength to the input points.

REFERENCES

- [1] [n. d.]. An RSMT implementation. https://github.com/shininglion/rectilinear_spanning_graph.
- [2] 2019. *ISPD '19: Proceedings of the 2019 International Symposium on Physical Design* (San Francisco, CA, USA). Association for Computing Machinery.
- [3] Yoshua Bengio, Andrea Lodi, and Antoine Prouvost. 2021. Machine learning for combinatorial optimization: a methodological tour d’horizon. *European Journal of Operational Research* 290, 2 (2021), 405–421.
- [4] Andrew E Caldwell, Andrew B Kahng, Stefanus Mantik, Igor L Markov, and Alex Zelikovsky. 1998. On wirelength estimations for row-based placement. In *Proceedings of the 1998 international symposium on Physical design*. 4–11.
- [5] Chris Chu. [n. d.]. FLUTE: Fast lookup table based technique for RSMT construction and wirelength estimation.
- [6] Alex Fallin, Aarti Kothari, Jiayuan He, Christopher Yanez, Keshav Pingali, et al. 2022. A Simple, Fast, and GPU-friendly Steiner-Tree Heuristic. In *2022 IEEE International Parallel and Distributed Processing Symposium Workshops (IPDPSW)*.
- [7] Maxime Gasse, Didier Chételat, Nicola Ferroni, Laurent Charlin, and Andrea Lodi. 2019. Exact combinatorial optimization with graph convolutional neural networks. *Advances in neural information processing systems* 32 (2019).
- [8] Maurice Hanan. 1966. On Steiner’s problem with rectilinear distance. *SIAM Journal on Applied mathematics* 14, 2 (1966), 255–265.
- [9] Chaitanya K Joshi, Quentin Cappart, Louis-Martin Rousseau, and Thomas Laurent. 2020. Learning the travelling salesperson problem requires rethinking generalization. *arXiv preprint arXiv:2006.07054* (2020).
- [10] Daniel Juhl, David M Warne, Pawel Winter, and Martin Zachariasen. 2018. The GeoSteiner software package for computing Steiner trees in the plane: an updated computational study. *Mathematical Programming Computation* (2018).
- [11] Andrew B Kahng, Jens Lienig, Igor L Markov, and Jin Hu. 2011. *VLSI physical design: from graph partitioning to timing closure*. Vol. 312. Springer.
- [12] Andrew B Kahng and Gabriel Robins. 1992. A new class of iterative Steiner tree heuristics with good performance. *IEEE Transactions on Computer-Aided Design of Integrated Circuits and Systems* 11, 7 (1992), 893–902.
- [13] Elias Khalil, Hanjun Dai, Yuyu Zhang, Bistra Dilkina, and Le Song. 2017. Learning combinatorial optimization algorithms over graphs. *Advances in neural information processing systems* 30 (2017).
- [14] Diederik P Kingma and Jimmy Ba. 2014. Adam: A method for stochastic optimization. *arXiv preprint arXiv:1412.6980* (2014).
- [15] Wouter Kool, Herke Van Hoof, and Max Welling. 2018. Attention, learn to solve routing problems! *arXiv preprint arXiv:1803.08475* (2018).
- [16] Jinwei Liu, Gengjie Chen, and Evangelina FY Young. 2021. Rest: Constructing rectilinear steiner minimum tree via reinforcement learning. In *2021 58th ACM/IEEE Design Automation Conference (DAC)*. IEEE, 1135–1140.
- [17] Azalia Mirhoseini, Anna Goldie, Mustafa Yazgan, Joe Wenjie Jiang, Ebrahim Songhori, Shen Wang, Eric Johnson, Omkar Pathak, Azade Nazi, et al. 2021. A graph placement methodology for fast chip design. *Nature* (2021).
- [18] Christopher Morris, Martin Ritzert, Matthias Fey, William L Hamilton, Jan Eric Lenssen, et al. 2019. Weisfeiler and leman go neural: Higher-order graph neural networks. In *Proceedings of the AAAI conference on artificial intelligence*.
- [19] Gi-Joon Nam, Charles J. Alpert, Paul Villarrubia, et al. 2005. The ISPD2005 Placement Contest and Benchmark Suite. In *Proceedings of the 2005 International Symposium on Physical Design*. Association for Computing Machinery.
- [20] Kenta Oono and Taiji Suzuki. 2020. Graph neural networks exponentially lose expressive power for node classification. *ICLR2020* 8 (2020).
- [21] Ladislav Rampásek, Michael Galkin, Vijay Prakash Dwivedi, Anh Tuan Luu, Guy Wolf, and Dominique Beaini. 2022. Recipe for a general, powerful, scalable graph transformer. *Advances in Neural Information Processing Systems* 35 (2022).
- [22] Jarrod A. Roy and Igor L. Markov. 2007. Seeing the Forest and the Trees: Steiner Wirelength Optimization in Placement. *IEEE Transactions on Computer-Aided Design of Integrated Circuits and Systems* (2007).
- [23] Khushro Shahookar and Pinaki Mazumder. 1991. VLSI cell placement techniques. *ACM Computing Surveys (CSUR)* 23, 2 (1991), 143–220.
- [24] Ashish Vaswani, Noam Shazeer, Niki Parmar, Jakob Uszkoreit, Llion Jones, Aidan N Gomez, Łukasz Kaiser, and Illia Polosukhin. 2017. Attention is all you need. *Advances in neural information processing systems* 30 (2017).
- [25] Yiu-Chung Wong and Chris Chu. 2008. A scalable and accurate rectilinear Steiner minimal tree algorithm. In *2008 IEEE International Symposium on VLSI Design, Automation and Test (VLSI-DAT)*. IEEE, 29–34.
- [26] Keyulu Xu, Weihua Hu, Jure Leskovec, and Stefanie Jegelka. 2018. How powerful are graph neural networks? *arXiv preprint arXiv:1810.00826* (2018).
- [27] Chengxuan Ying, Tianle Cai, Shengjie Luo, Shuxin Zheng, Guolin Ke, Di He, Yanming Shen, and Tie-Yan Liu. 2021. Do transformers really perform badly for graph representation? *Advances in Neural Information Processing Systems* (2021).
- [28] Summer Yue, Ebrahim M Songhori, Joe Wenjie Jiang, Toby Boyd, Anna Goldie, et al. 2022. Scalability and generalization of circuit training for chip floorplanning. In *Proceedings of the 2022 International Symposium on Physical Design*.
- [29] Zhiliu Zhang. 2016. Rectilinear Steiner Tree Construction. (2016).

A DATASET DESCRIPTION

dataset	netlist	#nets	degree	
			mean	median
ISPD2019 [2]	test1	1,199	10.93	4
	test2	30,471	7.31	4
	test3	3,498	5.49	4
	test4	60,104	3.86	3
	test5	5,467	5.89	4
	test6	76,169	7.32	4
	test7	152,171	7.33	4
	test8	228,146	7.33	4
	test9	380,151	7.34	4
	test10	380,151	7.34	4
ISPD2005 [19]	adaptec1	101,003	6.75	4
	adaptec2	98,138	7.19	4
	adaptec3	177,997	7.04	4
	adaptec4	179,689	6.70	4
	bigblue1	114,750	6.83	4
	bigblue2	203,712	6.15	4
	bigblue3	292,528	7.17	4

Table 5: Description of the netlists used for evaluation. Nets with degree smaller than 3 and larger than 64 are excluded.